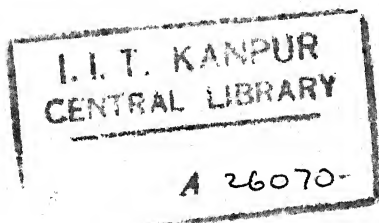


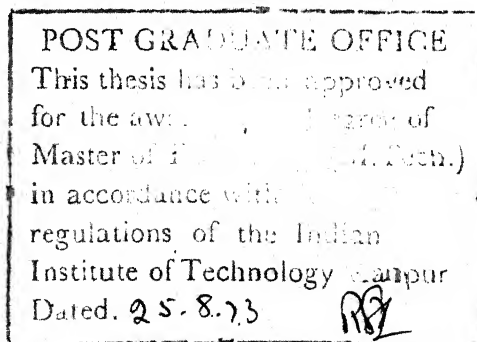
# CHARACTERIZATION OF EPITAXIALLY GROWN INDIUM PHOSPHIDE LAYERS

A Thesis Submitted  
In Partial Fulfilment of the Requirements  
for the Degree of  
MASTER OF TECHNOLOGY

By  
SUNIL B. PHATAK



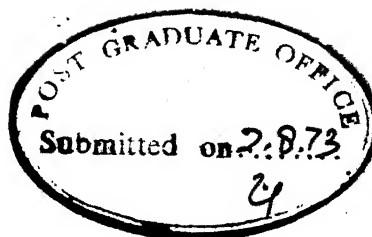
Thesis  
620.11  
P495



to the

INTERDEPARTMENTAL PROGRAMME IN MATERIALS SCIENCE  
INDIAN INSTITUTE OF TECHNOLOGY KANPUR  
JULY 1973

MS-1973-M-PAT-CHA



## CERTIFICATE

Certified that this work on "Characterization of Epitaxially Grown Indium Phosphide Layers" by Mr. Sunil B. Phatak has been carried out under my supervision and that this has not been submitted elsewhere for a degree.

DR. R. SHARAN  
Assistant Professor  
Department of Electrical Engineering  
Indian Institute of Technology  
Kanpur.

<p>POST GRADUATE OFFICE This thesis has been approved for the award of the degree of Master of Technology (M.Tech.) in accordance with the regulations of the Indian Institute of Technology Kanpur Dated. 25.8.73</p>
--



## ACKNOWLEDGEMENTS

I am grateful to Dr. R. Sharan for suggesting this problem to me and guiding me in every phase of the work.

I am indebted to Professor E.C. Subbarao, Mr. M.M. Hasan and Mr. Gurucharan Singh for the invaluable help they have given me.

My special thanks go to Mr. Mohammed Hamiuddin, my colleague, who not only helped me throughout this work but also maintained a healthy and creative atmosphere.

I should like to thank Mr. R.N. Srivastava for his excellent typing.

Finally, I take this opportunity to thank all my comrades and friends without whose timely and much needed help this work could not have been done.

July, 1973.

*S.B. Phatak*

S.B. PHATAK

## CONTENTS

## LIST OF FIGURES &amp; TABLES

v

## SYNOPSIS

vi

## CHAPTER

1	INTRODUCTION	1
	1.1 An Overview	1
	1.2 Properties of III-V compounds	3
	1.2.1 The Energy bands	3
	1.2.2 Structure & X-ray diffraction	6
	1.2.3 Optical absorption near the fundamental edge	8
	1.2.4 Electrical properties of thin films	9
2	GROWTH	10
	2.1 Choice of the growth technique	10
	2.2 A description of the apparatus	12
	2.2.1 Hydrogen purifier	12
	2.2.2 Control console	13
	2.2.3 Epitaxial reactor	14
	2.3 Epitaxial growth procedure	15
	2.4 An account of the experimental runs	17
3	CHARACTERIZATION	20
	3.1 Preamble	20
	3.2 Visual inspection	20
	3.3 Thickness measurement	21
	3.4 Dislocation density measurement	24
	3.5 X-ray measurements	26
	3.6 Band-gap measurement	27
	3.7 Conductivity-type and resistivity	29
4	SOME STUDIES ON Si-InP HETEROJUNCTIONS	31
	4.1 Purpose of this study	31
	4.2 Fabrication of heterojunction diodes	32
	4.3 Measurements	35
5	EPILOGUE	39
	5.1 Discussions & Conclusions	39
	5.2 Suggestions for further work	44
	REFERENCES	47

## I TABLE OF FIGURES

FIG.NO.		Page
1	ENERGY BAND DIAGRAMS FOR GaAs & InP	5
2	FIRST BRILLOUIN ZONE OF THE ZINC-BLENDE LATTICE	7
3	VELOCITY-FIELD CHARACTERISTICS FOR GaAs & InP	7
4	SCHEMATIC REPRESENTATION OF EPITAXIAL GROWTH APPARATUS	11
5	CROSS-SECTION OF CLEAVED SAMPLE	22
6	ANGLE-LAPPED SAMPLE FROM RUN NO. 16	25
7	INFRA-RED ABSORPTION OF EPITAXIAL LAYERS	28
8	FABRICATION OF HETEROJUNCTION DIODE	33
9(a), (b) & (c)	I-V CHARACTERISTICS OF HETEROJUNCTION DIODES	36
9(d), (e) & (f)	I-V CHARACTERISTICS OF N-TYPE Si - N-TYPE InP HETEROJUNCTION (RUN NO. 13)	37
9(g)	I-V CHARACTERISTICS OF N-TYPE Si - N-TYPE InP CHIP (RUN NO. 13) MOUNTED ON HEADER	38

## LIST OF TABLES

I	DATA FROM EXPERIMENTS	39
II	X-RAY ANALYSIS BY DEBYE-SCHERRER TECHNIQUE	46

## SYNOPSIS

CHARACTERIZATION OF EPITAXIALLY  
GROWN INDIUM PHOSPHIDE LAYERS

A thesis submitted by

Sunil B. Phatak

to the

Interdepartmental Programme in Materials Science,  
Indian Institute of Technology, Kanpur

for the Degree of

M.Tech. in Materials Science

July, 1973

This work is concerned with characterization of epitaxial layers of InP. These layers were grown by vapor phase chemical transport method using In and  $\text{PCl}_3$  as starting materials and hydrogen gas as the transport agent.

Thickness of these layers was measured by the angle-lap and stain method. Chemical etching was used for estimating the dislocation density.

Debye-Scherrer powder method and Laue back-reflection technique were used for measuring the lattice-parameter and to reveal the crystalline perfection of the layers respectively.

The fundamental absorption edge was found to be in the range 1.24 - 1.40 eV and this agrees with the previously reported values.

The layers are n-type, although no intentional doping was done. Resistivity measurements indicate that the samples are rather pure; the carrier density ( $N_D - N_A$ ) being of the order of  $10^{14} \text{ cm}^{-3}$ .

Some investigations on Si-InP heterojunctions are also reported.

## CHAPTER ONE

### INTRODUCTION

#### 1.1 An Overview

In recent years, there has been a growing awareness of the need to study the relation between the structure and properties of materials. In particular, this has been the case with the new families of compound semiconductors. The extensive research devoted to the physics of compound semiconductors during the past decade has led to a more complete understanding of the physics of solids in general. This progress was made possible by significant advances in materials preparation and characterization techniques. The availability of a large number of compounds with a wide variety of different and often unique properties enabled the investigators not only to discover new phenomena but to select optimum materials for definitive experimental and theoretical work. It has thus been possible to prepare materials with desired properties which optimize the performance of any given device.

As an example, we cite the Transferred Electron Devices (TED's) which were developed following the discovery by J.B. Gunn that microwave oscillations can be generated in bulk semiconductors<sup>(1)</sup>. Gunn first observed this bulk-effect in GaAs and InP; two of the semiconductors known as "III-V

Compounds". At this point, perhaps, it is pertinent to trace the history of these III-V compound semiconductors. H. Welker appears to have been the first to realize the importance of these materials as an entirely new family of semiconductors. He pointed out that some of them have some very interesting properties, e.g. high carrier mobilities, and that they are closely related to the column IV elemental semiconductors. Among these compounds, our interest in the present work is mainly in indium phosphide.

Although it was realized rather early (in late 1950's) that InP will be a very useful material, very little effort was put on it because another member of the family, GaAs, appeared to be more suitable for device fabrication. This was due to several factors like its higher band-gap, higher electron mobility<sup>(2)</sup> and, perhaps the most important of all, the ease of preparation. The discovery of Gunn-effect gave a further impetus to the development of GaAs and InP was relegated to a secondary position. However, in 1970 Hilsum<sup>(3)</sup> discovered that a three-level transferred electron device could give much better performance than GaAs devices in which a two-level electron transfer mechanism is operative. It was also found out that certain ternary systems and InP possess the necessary energy-level structure. Following this discovery, quite a few laboratories around the world are engaged in this field, but since the technology of InP is not yet very well developed, the present work was undertaken.

After a preliminary screening of all the possible methods of growing epitaxial layers of InP, the vapor phase chemical transport method was chosen. The advantages of this method and further details of the technique are given in Chapter 2. But before that it is necessary to discuss the properties of III-V compound semiconductors in some detail.

Ever since Welker published his findings, the interest in these compounds has increased. At intervals, as data accumulated, several review articles<sup>(4-7)</sup> were published and specialized monographs<sup>(8-12)</sup> were devoted to this field. Today we find that these materials have been rather thoroughly investigated. Hence, in the following lines, only those properties of III-V compounds which are of major importance and are relevant to this work are described.

## 1.2 Properties of III-V Compounds

### 1.2.1 The energy bands:

Keeping in mind the motive behind this work, it is only natural that a discussion of the transferred electron effect should precede other matters.

When a voltage of sufficient magnitude is applied to two ohmic contacts placed on a bar of GaAs or InP, it gives rise to current oscillations in the microwave region. The primary reason for this oscillation is the transfer of electrons from a low lying conduction band valley to a higher conduction band



valley, under the influence of the high electric field. It is due to this reason that a device based on this effect is called a Transferred Electron Device or TED. TED's are also known as Gunn effect devices, since Gunn was the first to observe these oscillations.

The basic mechanism of transfer of electrons in GaAs and InP is slightly different in as much as in GaAs only two conduction band valleys are involved whereas in InP three conduction band valleys are involved. The  $E(k)$  diagrams of GaAs<sup>(13)</sup> and InP<sup>(14)</sup> are shown in Fig. 1, where  $\Gamma$ , X and L are specific notations used to denote the various symmetry points in the Brillouin zone. The Brillouin zone of a zinc-blende structure, which is a truncated octahedron is shown in Fig. 2. Here  $\Gamma$  denotes the centre of the Brillouin zone, X denotes the intersection of the  $[1\ 0\ 0]$  axes with the zone boundary and L denotes the intersection of the  $[1\ 1\ 1]$  direction with the zone boundary.

In both GaAs and InP, at small applied fields all the conduction band electrons are at the  $\Gamma$  level. However, at higher fields, these electrons gain energy and momentum until some of them are transferred to the next higher valley. Since the mobility in this valley is much less than that in the  $\Gamma$  valley, a region of negative differential mobility results at these high fields.

In GaAs<sup>(15)</sup>, this electron transfer process from  $\Gamma$  to X valleys is comparatively slow and at any particular

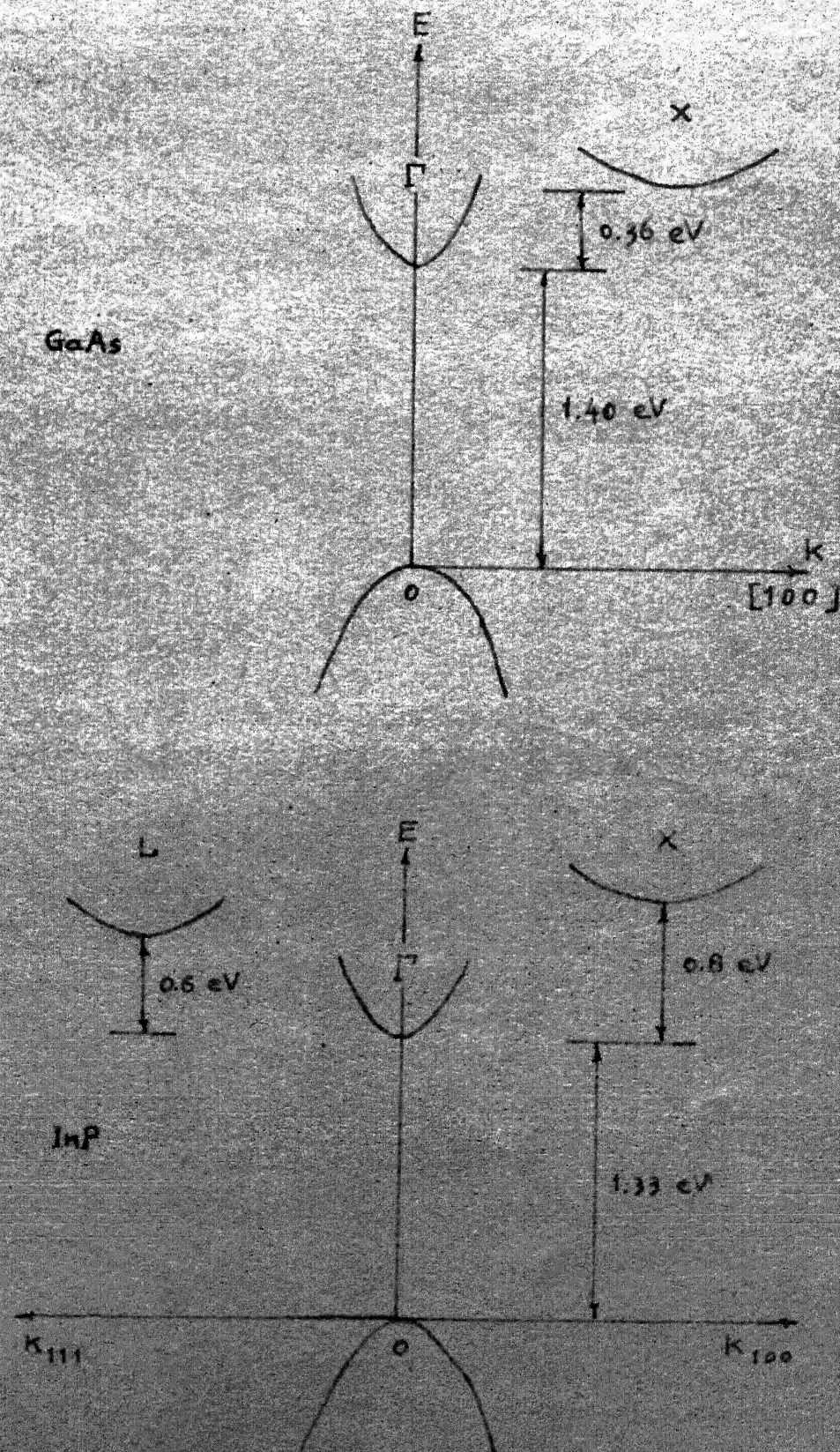


FIG. 1 ENERGY BAND DIAGRAMS FOR GaAs AND InP.

voltage above threshold, the contribution from the  $\Gamma$  valley to the total current is large. As a result, the peak-to-valley current ratio is low (Fig. 3) and the negative resistance region is not very pronounced.

To increase the peak-to-valley ratio, therefore, an electron transfer is needed which proceeds rapidly as the field is increased. This can be achieved if the coupling between the  $\Gamma$  and X levels is weak - not strong as in GaAs. The problem with such a weakly coupled system is that some  $\Gamma$  electrons would acquire energies high enough to cause impact ionization, resulting in breakdown of the material at low field strengths. An additional energy dissipating mechanism is required to avoid this breakdown, and usually this can be provided in a third energy level.

InP possesses such an energy level structure, as Fig. 1(b) shows. Here, the  $\Gamma$  level is weakly coupled to the L level, but strongly coupled to the X level to prevent breakdown. Strong coupling between X and L levels and weak coupling between L and  $\Gamma$  levels insure that, under normal operating conditions, electrons concentrate at the L level. The improved peak-to-valley ratio of InP is to be contrasted with that of GaAs in Fig. 3.

### 1.2.2 Structure and X-ray diffraction:

As mentioned above, the III-V semiconductors have a zinc-blende structure. This is very similar to the diamond



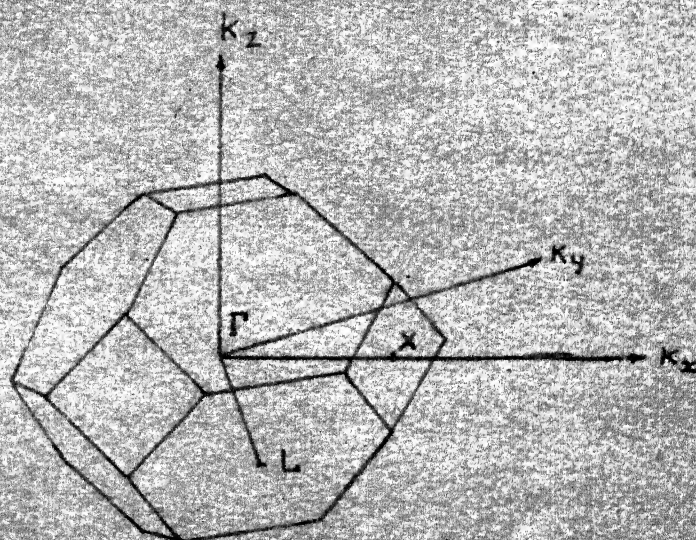


FIG. 2. FIRST BRILLOUIN ZONE OF THE ZINC-BLENDE LATTICE.

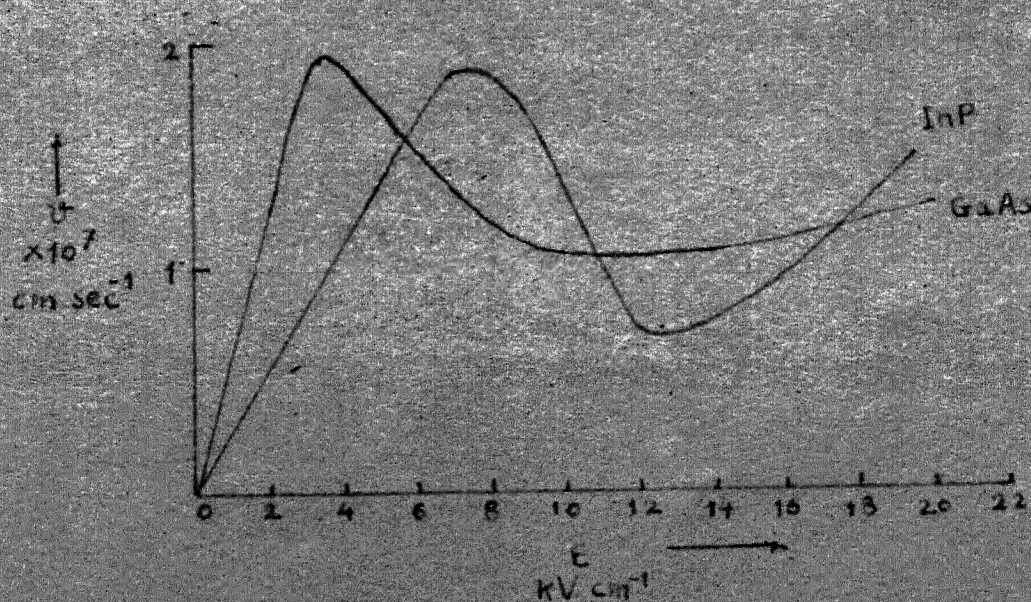


FIG. 3. VELOCITY-FIELD CHARACTERISTICS FOR GaAs AND InP.

structure with the difference that in the latter all the atoms are alike. The zinc-blende lattice can be thought of as two interpenetrating f.c.c. sublattices, where one sublattice (say A) consists entirely of group III atoms and the other (say B) of only group V atoms. The sublattices A and B are oriented parallel to and are displaced from, each other by a quarter of the f.c.c. body diagonal.

In an X-ray diffraction experiment, the diffraction maxima observed with such a structure are similar to those obtained with a simple f.c.c. lattice. All the lines of the f.c.c. lattice are present, the only difference being in the intensity of these lines. The diamond lattice, with all like atoms, gives a diffraction pattern in which some of the f.c.c. lines are missing because the interference in diffracted X-rays from certain positions is destructive. In the zinc-blende lattice this cancellation is not complete because of the presence of two kinds of atoms and hence all the f.c.c. lines are present.

This fact has been made use of in lattice parameter measurements by Debye-Scherrer powder patterns, as described in Section 3.4.

### 1.2.3 Optical absorption near the fundamental edge:

The measurement of the intrinsic absorption of semiconductors is a powerful tool for studying the energy band structure of solids. The measurement of the fundamental absorption edge (lowest-energy absorption edge which corresponds

to the threshold for electron transitions between the highest nearly filled band and the lowest nearly empty band) yields the energy band gap,  $E_g$ , and the nature (direct, indirect) of the transitions involved. The absorption is very small for photon energies less than  $E_g$  and increases by several orders of magnitude at higher photon energies.

The most direct way of observing the fundamental edge is from transmission measurements, and this was the procedure used in this work. Further details of this technique are given in Section 3.5.

#### 1.2.4 Electrical properties of thin films:

The electrical properties of III-V compound films depend to a large extent on their crystalline perfection, dislocations and other defects<sup>(6)</sup>.

For doping, normally Zn and Cd are used for p-type doping and Se, Te and S for n-type doping. It has been also found<sup>(16)</sup> that oxygen acts as a donor in InP. This fact has important consequences in our work since invariably hydrogen gas, used as transport agent, contains oxygen as an impurity and this leads to n-type doping of InP.

The mechanism by which oxygen acts as donor in InP is, however, not well established.

## CHAPTER TWO

GROWTH2.1 Choice of the Growth Technique

In this work, indium phosphide epitaxial layers were grown by the open tube vapor phase chemical transport method. This method has the following advantages:

1. It provides good control of the chemical composition, homogeneity, crystalline perfection, and impurity concentrations in the epitaxial layers.
2. All the starting materials ( $\text{PCl}_3$ , indium, and hydrogen) can be readily obtained in sufficiently pure form.
3. Although  $\text{PCl}_3$ , because of its poisonous nature, and hydrogen, due to its explosive properties, present hazards in experimental operation, these can be easily circumvented by proper care in the design of the apparatus.
4. The apparatus itself is simple in design and rather easy to construct.

The growth apparatus is schematically depicted in Fig. 4.

The major sections in this figure are:

1. Hydrogen purifier
2. Control console
3. Epitaxial reactor.

All the pieces of equipment, except the furnace, were fabricated in the Institute. Further details of fabrication



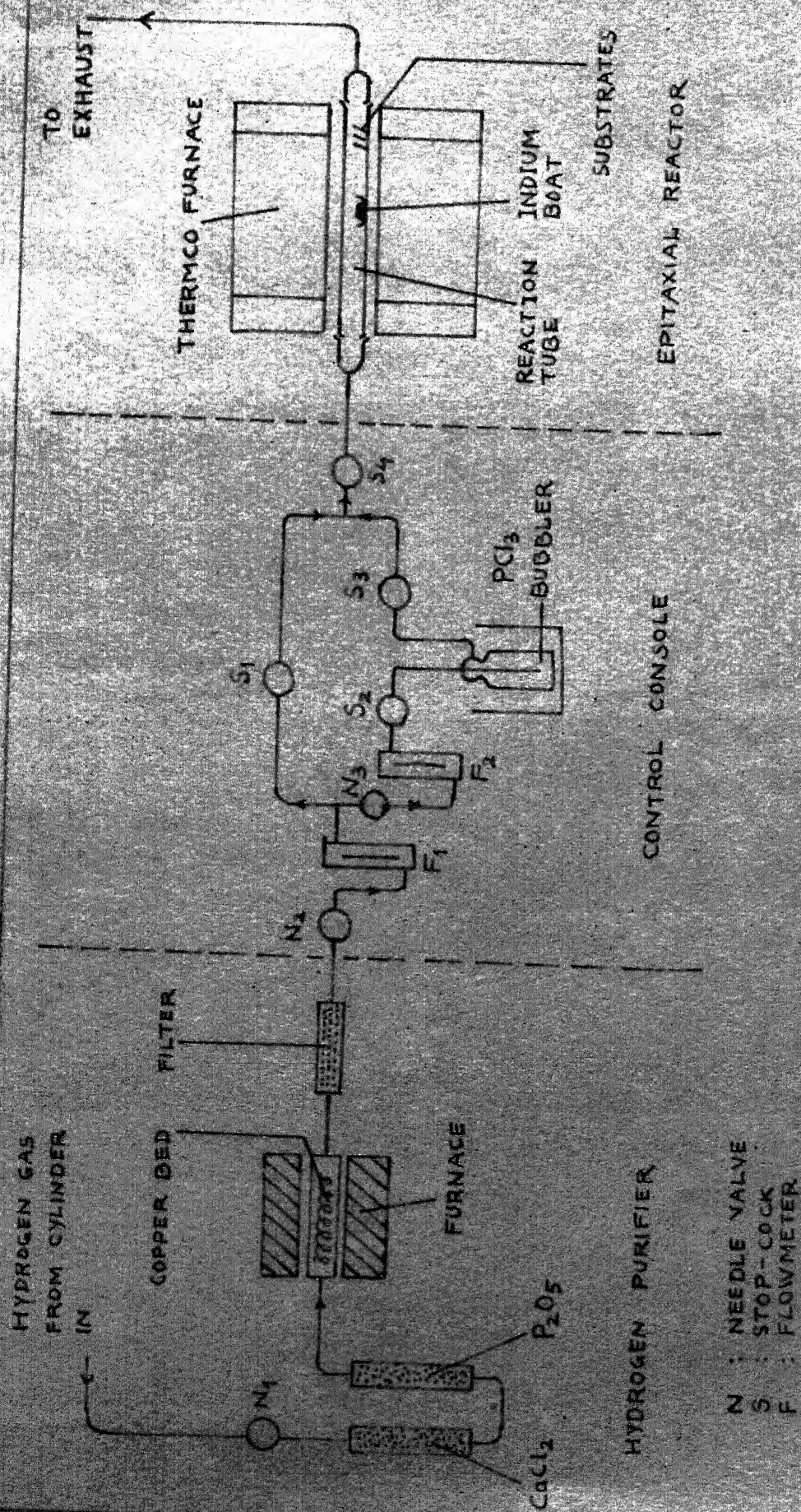


FIG.4. SCHEMATIC REPRESENTATION OF EPITAXIAL GROWTH APPARATUS



are given in Reference 17.

This apparatus was installed in the ~~clean~~-rooms of the Integrated Circuits Lab.

## 2.2 A Description of the Apparatus

### 2.2.1 Hydrogen purifier:

Hydrogen gas used in this work was obtained from Indian Oxygen Ltd., and the main impurities in this supply are  $O_2$ ,  $N_2$ ,  $CO_2$ ,  $Cl_2$ , and moisture. Among these, the impurities which change the electrical properties of InP and thus are electrically active are oxygen and moisture. The removal of these is accomplished by passing hydrogen through a train of several absorbers where these impurities are absorbed.

First in the purification train comes a pyrex tube filled with anhydrous calcium chloride which absorbs a part of the water vapor. Then hydrogen is allowed to pass through phosphorous penta oxide which is a very efficient absorber of moisture. Since  $P_2O_5$  is in a finely powdered form, it has to be mixed with glass wool before filling in the pyrex tube so that it may not choke the flow of gas. Hydrogen coming out of these two tubes is almost free of water vapor.

To remove oxygen from the gas stream, it is passed over a 12" bed of copper wire put inside a quartz tube maintained at a temperature of approximately  $500^\circ C$ . Quartz tube has been used since pyrex softens due to prolonged exposure to such high temperatures. The copper wire was obtained from electrical

flexible wires and then cut into small pieces. The thin wire has a high surface to volume ratio and ensures efficient removal of oxygen through formation of oxide. It is thought that copper can remove oxygen upto a maximum factor of  $10^{-6}$ .

Next this hydrogen is passed through 10" column of densely packed glass wool to make it free of any particles and is then fed to the control console.

### 2.2.2 Control console:

This consists of two needle valves, flow meters, several pyrex stop-cocks, a  $\text{PCl}_3$  bubbler and the associated pyrex glass and PVC tubing.

The flowmeters are rotameter type and were obtained from Instrumentation Engineers Ltd., Hyderabad. They are assembled in such a manner that both the total flow of hydrogen and the amount of hydrogen bubbling through  $\text{PCl}_3$  could be monitored. The stop-cocks and needle valves can control the hydrogen flow so that either all of it can be fed directly to the reaction tube, or all of it can be passed through the bubbler, or a part of it can be diverted to the bubbler and the rest of it can go directly to the reaction tube. These operations are necessary for purging, source saturation, and during normal course of growth respectively.

Care was taken to make use of pyrex glass tubing to a maximum and to use PVC tubing only when necessary to minimize the possible contamination and leakage of hydrogen.

All these components were mounted on a movable trolley made of angle-iron and based on four castor wheels. When not in use, this trolley could be moved away from the epitaxial reactor and kept in a safe place. The hydrogen purifier was also located on this trolley.

### 2.2.3 Epitaxial reactor:

This consists of a 25 mm ID quartz reaction tube and the Thermco diffusion furnace. The reaction tube contains an indium boat located in the central part and the substrates on a quartz substrate holder kept down stream.

The furnace has a long (16") central zone, and two end zones the temperatures of which can be maintained to within  $\pm 50^{\circ}\text{C}$  of the central zone temperature, which itself can be heated to  $1400^{\circ}\text{C}$ . The overall temperature control in this furnace is to within  $\pm 0.25^{\circ}\text{C}$ , obtained through the use of SCR Circuitry. Since the temperature profile of this furnace was known, the substrates could be kept at any desired temperature by changing the position of substrate holders along the tube axis.

Ground-glass taper joints were provided at both the ends of the reaction tube through which it could be connected to the control console at the inlet end and to the clean-room exhaust at the outlet end.

The substrates employed for depositing InP were of Ge, Si, quartz and sapphire. With Ge and Si, both the conductivity

types and different conductivities were used. Quartz and sapphire substrates were mainly for use in the infra-red measurements and this is described in details in Section 3.4.

### 2.3 Epitaxial Growth Procedure

The growth of InP epitaxial layers was carried out in the following steps:

1. Weighed quantities of In metal, after cutting it into small pieces and cleaning thoroughly, were put in a perfectly cleaned quartz boat made specially for this purpose and then inserted in the reaction tube. The In boat was kept in the central zone of the furnace.
2. Substrates were put in the slotted quartz substrate holders and were inserted in the reaction tube to a particular position corresponding to a known and predetermined temperature.
3. The tapered joints were connected to the reaction tube. Then the inlet-end tapered joint was connected to the pyrex tube coming from the trolley with the help of a small length of PVC tubing and another length of PVC tubing was used to connect the outlet-end tapered joint to the clean-room exhaust. The system in this situation is open to the atmosphere only through the exhaust and, when hydrogen gas is turned on, is completely leak-tight.
4. Furnace containing the copper bed was switched on and the power input was increased gradually. This furnace takes

about 60 minutes to reach the desired temperature of 500°C.

5. Hydrogen flow in the reaction tube was started for purging the air in the system. Large quantities of hydrogen, upto 1 l/min, were passed in this stage to ensure that the reaction tube is totally free of any air when the Thermco furnace is on. This flushing is necessary to avoid the danger of explosion. Further, air may oxidise the indium and substrates at elevated temperatures. During flushing the  $\text{PCl}_3$  bubbler is completely shut-off.
6. After flushing the reaction tube, for about 10-15 minutes, the furnace is switched on with the temperature controls set at the necessary values. In all the runs, the central zone temperature was maintained at 800°C and that of the end zone at 750°C. It takes about forty minutes for the temperature to stabilize and during this period the hydrogen flow rate is kept at about 100 cc/min.
7. After the temperature has stabilized, hydrogen is allowed to flow through  $\text{PCl}_3$ . This flow can be regulated accurately with the help of flowmeter  $F_2$  and needle valve  $N_3$ . Normally  $\text{PCl}_3$  was kept at room temperature. In some runs the  $\text{PCl}_3$  bubbler was surrounded by an ice jacket. In such events, a fresh supply of ice has to be fed to the jacket to keep the flux temperature (i.e. the temperature of  $\text{PCl}_3$ ) constant.
8. During the first few minutes phosphorous, liberated by the reaction of  $\text{PCl}_3$  with  $\text{H}_2$ , reacts with In to form a

thin layer of InP over the molten metal. This period is known as saturation period and epitaxial growth of InP commences only after the saturation is over. During this period, a major part of  $H_2$  flow is diverted to the  $PCl_3$  bubbler.

After the saturation of In is complete, the flow of hydrogen is again changed with the help of the needle valves. The ratio of the amount of hydrogen going directly to the reaction tube to the amount passing through  $PCl_3$  can thus be varied, and was kept between zero and 3. This period is the actual growth period and its duration was varied from 1 hr. to 3 hrs.

At the end of the desired growth-time, the furnace is switched off and flow of  $H_2$  through  $PCl_3$  is discontinued after about 5 minutes. A small quantity of  $H_2$  is allowed to flow till the furnace has cooled down appreciably. Then the  $H_2$  flow is also shut-off.

Samples are taken out when the furnace has finally cooled down to room temperature and are subjected to a visual inspection immediately.

#### 2.4 An Account of the Experimental Runs

In all, 17 growth runs were made out of which 15 were of the nature described above. In these 15 runs it was observed that the chances that growth of InP could take place were only

when the substrate temperature was within the range 610 to 690°C. This, in general, is consistent with the results of past workers. Further details of these runs are summarized in Table I.

Two runs, run numbers 14 and 15, were of a specialized nature. These were designed to find out whether any phosphorous or indium deposition or diffusion into substrates takes place prior to the deposition of InP. In run number 14,  $\text{PCl}_3$  was not used at all and only indium was heated to 800°C in the hydrogen stream. Although n-type Si and Ge substrates did not show any change in their conductivity types, eliminating the possibility of indium diffusion and consequentially a p-n junction formation, however, some indium metal deposits were indeed found on these substrates and also on p-type substrates. This run was continued for 50 minutes from switching the Thermco furnace on, which is the time period available for indium to deposit on the substrates before  $\text{PCl}_3$  flow is turned on in normal runs. The indium deposits were in the form of extremely small specks bunched together to form small clusters. These clusters were distributed over the substrate surface without any apparent regularity.

Run number 15 did not use any indium and only  $\text{PCl}_3$  and hydrogen were allowed to flow in the reaction tube for 30 minutes. Again, the p-type Ge and Si substrates did not change their conductivity types and there were no phosphorus deposits on the substrate surfaces.

The reason for the conductivity type to remain unchanged in both the runs is the extremely small diffusion constants of phosphorous and indium at the low values of substrate temperatures employed.

These two runs were necessitated by the following reasons:

1. During mechanical polishing of the epitaxial layers it was observed that the layers peel off the substrates very easily, showing poor adhesion between the substrates and the epitaxial layers. It was thought that this might happen in case there is an intermediate indium or phosphorous layer.
2. In the studies of InP - Si heterojunctions it was pointed out that the observed rectifying behaviour could be obtained with the following structure:

If there is a shallow p-n junction formation due to diffusion of indium or phosphorous in n-type or p-type substrates respectively, followed by a thin layer of metallic indium over which deposits the InP. Then this structure can show rectifying properties due to the shallow junction, with the indium layer providing just an ohmic contact on the diffused side, and the InP layer merely adding some series resistance.

As is clear from the results of runs 14 and 15, such a possibility can immediately be excluded. The only effect that the indium deposits could have was in forming additional interface states which can change the heterojunction properties.



## CHAPTER THREE

CHARACTERIZATION3.1 Preamble

The evaluation of epitaxial films presents many problems that are absent in the analysis of bulk semiconductors. Although the methods used in this work are simple in theory<sup>(20)</sup>, a great deal of care is needed to use them in actual practice. An obvious problem is that of handling and storing the samples. Sharp-nosed tweezers were used for handling the samples so that the damage to the surfaces could be minimized. Great care was exercised, since the samples tended to break at the slightest pressure. Petry dishes, lined with soft Whatman analytical filter papers were used for storing the samples.

3.2 Visual Inspection

The as-grown layers, freshly removed from the epitaxial reactor were visually inspected through a low magnification stereo microscope (Bausch and Lomb, Stereozoom 7). The purpose of these observations was to see the colour, the surface texture, surface inclusions etc. and to reveal the irregularities in the films, if any, and the presence of whiskers which might give a clue to the growth processes.

The colour of the deposited layers was dark gray with a tary lusture. Often phosphorous and, sometimes, indium deposits

could be seen. In cases where whisker growth was observed, the size and shape of whiskers differed from sample to sample in the same run, and also in different runs.

Another feature of the thicker layers was the presence of holes which created some complications during polishing operations.

### 3.3 Thickness Measurement

For measuring the thickness of the epitaxial layers, the angle-lap method was employed. In some runs, cleaved samples could be obtained and angle lapping was not necessary as, then, the transverse cross-section of the sample could readily be observed under a microscope (Fig. 5).

For angle-lapping, mechanical polishing was done starting with 5  $\mu\text{m}$  alumina lapping powder. The samples were mounted on a  $10^\circ$  lapping fixture with the help of apiezon wax and were then lapped on ground-glass plates using water as a lubricant. During this abrasive lapping, the odour of burnt phosphorous was quite perceptible and was probably due to  $\text{PH}_3$  liberated by decomposition of  $\text{InP}$ .<sup>(18)</sup>

Next, the sample holder was thoroughly cleaned and transferred to another glass plate for lapping with 1  $\mu\text{m}$  lapping powder. In some cases a polishing wheel was also employed for this purpose and then a slurry of the lapping powder in distilled water was poured on the rotating wheel. The speed of

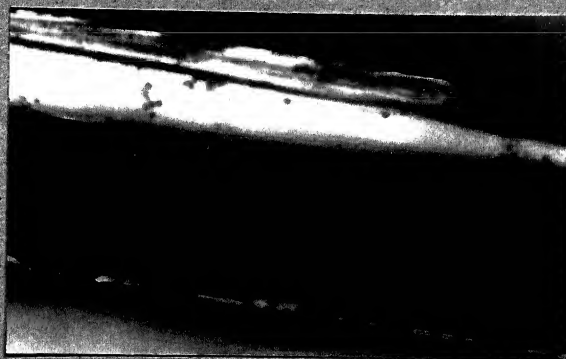


FIG. 5 CROSS-SECTION OF CLEAVED SAMPLE

the wheel was regulated to about 120-150 rpm to avoid any shock to the layers.

After this, the samples were removed from apiezon wax by heating the sample holder and then were cleaned with trichloroethylene, acetone and, finally, methanol.

These samples were then etched to delineate the substrate-layer boundary. The etchant used<sup>(16)</sup> was: potassium hydroxide (6 g) + potassium ferricyanide (4 g) in 50 ml water. Etching time was upto five minutes at room temperature.

Peeling-off of the epitaxial layers from the substrates presented a major problem during this process. Some of the layers tended to peel-off as soon as they were lapped, so that a hazy boundary line was obtained on the lapped part and hence the thickness could not be measured accurately. The reason for this is a lack of good adhesion between the substrate and the epitaxial layer. This may be due to several reasons:

1. Substrate surface preparation:

If the substrate is not completely clean or smooth and if there are deposits and irregularities on the surface, it may give rise to an uneven growth and thus lead to poor adhesion. All due care was therefore taken in the preparation of substrates and these substrates were the best that could be obtained in this laboratory.

2. Indium deposition:

In the beginning of a run, flow of hydrogen is started



even before the furnace is switched on and this flow then continues throughout the duration of the run. As explained before in Section 2.4, there may be some deposits of indium before InP starts getting deposited on the substrates.

### 3. Lattice mismatch:

This is a case where the substrate may be ideally clean and there is no deposit prior to the epitaxial growth, but where the lattice parameters of substrate and the epitaxially grown crystal differ by a large extent. In this case the dislocation density near the substrate-layer interface will increase tremendously and the epitaxial layers will peel off under shear.

In face of all these difficulties, a procedure which could be used with limited success was to polish the sample with extreme gentleness.

An interesting method for estimating the thickness was discovered while lapping a thick layer from run number 16. In this case, a part of the layer peeled off, leaving the deposit on the edges of the sample intact and this part could be used for estimation of thickness (Fig. 6).

#### 3.4 Dislocation Density Measurement

The layers or parts of the layers which survived mechanical polishing were then polished chemically and preferentially etched for revealing dislocation pits. The chemicals<sup>(19)</sup>



FIG. 6. ANGLE-LAPPED SAMPLE FROM RUN NUMBER 16.

used for this purpose were:

Caro's acid, i.e.  $\text{H}_2\text{SO}_4 + \text{H}_2\text{O}_2 + \text{H}_2\text{O}$  (4 : 1 : 1) for polishing, and

N  $\text{FeCl}_3$  + 5N HCl for dislocation etch pitting on (1 1 1) planes.

The dislocation density varied between  $10^5$  to  $10^9 \text{ cm}^{-2}$ . These measurements could be made only on some small parts of the surfaces and hence are only approximate.

### 3.5 X-ray Measurements

X-ray techniques were used for two purposes:

1. Lattice parameter measurements were done using Debye-Scherrer powder photographs. The material for this was obtained from peeled-off layers, substrate holders and from walls of the quartz reaction tube. All these specimens give consistent results and are tabulated in Table I.  $\text{CuK}_\alpha$  radiation was used and the exposure time was from 4-6 hours.
2. Crystalline perfection was checked by Laue back-reflection photograph of one substrate-layer combination taken in such a way that the epitaxial layer was facing the X-ray beam. This epitaxial layer, at least at that spot, possesses high crystalline perfection. Here, Cu target was used and the exposure time was 3 hours.

### 3.6 Band-gap Measurement

Optical absorption of thin layers in the near infra-red region was used in order to determine the fundamental absorption edge of the material. The spectra have to be obtained on substrate-epitaxial layer composites since the layers being very thin present handling problems. Hence, the substrate has to be transparent in the wavelength range of interest. For this reason, single crystal sapphire and quartz wafers were used as substrates. The measurements were carried out on a Cary 14 spectrophotometer.

The samples were mounted on thick paper in which windows of proper size were cut. This paper was then glued to the sample holders with the help of cello tape.

Measurements indicate that the band-gap of this material lies in the range 1.24-1.42 eV. The infra-red spectra are shown in Fig. 7(a), (b) and (c). In Fig. 7(b), the small shoulder in the region AB may be due to transitions between the valence band and an impurity level. The donor impurity has not been identified, but typical values of donor excitation energies can be calculated approximately by assuming a hydrogenic impurity model. Taking the effective mass of electrons<sup>(20)</sup> to be 0.078, we find that  $E_d \simeq 0.007$  eV.

The sudden change of absorption from B to C can certainly be attributed to the fundamental absorption edge. The reported value<sup>(14)</sup> of band-gap at 300°K is 1.33 eV.



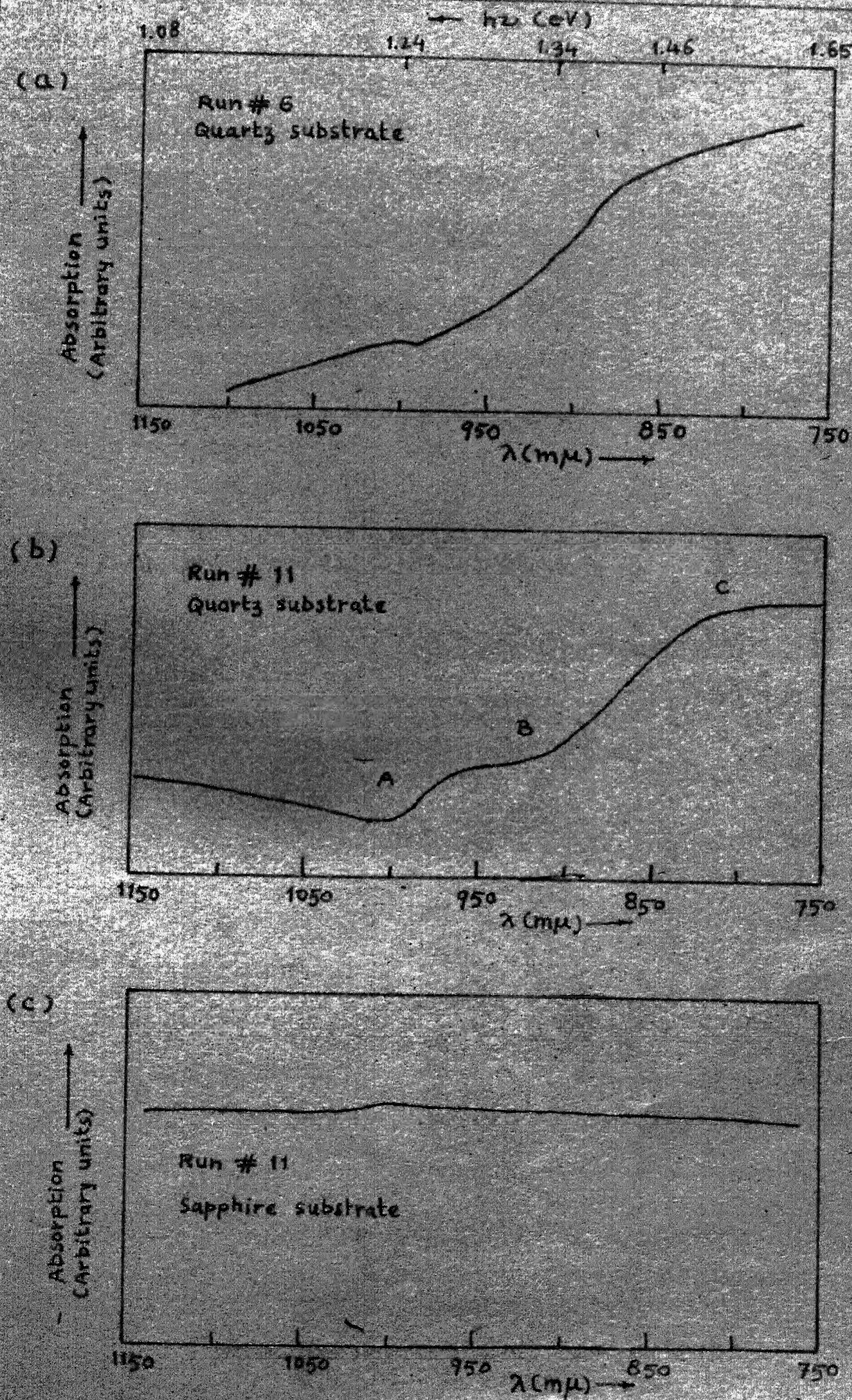


FIG. 7. INFRARED ABSORPTION OF EPITAXIAL LAYERS

Fig. 7(c) shows that all the radiation falling on this sample is being absorbed. This indicates that there is an opaque metallic (probably indium) layer, sandwiched in-between the substrate and the epitaxial layer.

### 3.7 Conductivity Type and Resistivity

The type of conductivity (n-type or p-type) was determined with the help of a "hot-point probe". All the samples checked were n-type without any exceptions, although no intentional doping was done.

The resistivity (inverse of conductivity) was measured with a Four-point probe Model A-4 with a probe head type PH-71 made by OSAW, India. The probe spacing,  $a$ , is 1.5 mm. The resistivity is calculated by using the formula

$$\rho = \frac{\pi}{\ln 2} t \frac{V}{I}, \quad \text{ohm-cm} \quad t = \text{thickness}$$

where  $V$  is the voltage developed between the two central probes when a current  $I$  (in amp.) is passed through the outer probes. The values obtained are  $1.39 \times 10^3$  ohm-cm in runs 12 and  $5.95 \times 10^3$  ohm-cm in run 2, and  $1.32 \times 10^4$  ohm-cm in run 6. There is a large variation in these values although the sources of impurities are expected to be the same. These variations, probably, are due to difference in surface quality of different samples.

Despite this, the high values of resistivity indicate that the material is rather pure or that compensation is taking place to a great extent. The carrier concentration can be estimated

as follows:

The intrinsic carrier concentration,  $n_i$ , is given by,

$$n_i^2 = N_c N_v e^{-E_g/kT}$$

where  $N_c = 2(2\pi m_n^* kT/h^2)^{3/2}$ , and

$$N_v = 2(2\pi m_p^* kT/h^2)^{3/2}$$

Taking the effective masses<sup>(21)</sup> of electrons as  $m_n^* = 0.078 m_0$ , and of holes as  $m_p^* = 0.7 m_0$ ,  $n_i$  comes out to be  $5.74 \times 10^6 \text{ cm}^{-3}$  at 300°K.

For estimating the electron concentration in doped semiconductors, we make use of the expression.

$$\frac{1}{\rho} = q n \mu_n, \text{ where } \mu_n \text{ is the electron mobility, hence, } n = \frac{1}{\rho q \mu_n}$$

Taking  $\mu_n = 4500 \text{ cm}^2 \text{ V}^{-1} \text{ sec}^{-1}$ , we obtain the electron concentration as:

Run 12 and 13 (140 ohm-cm) :	$9.926 \times 10^{12} \text{ cm}^{-3}$
Run 2 (610 ohm-cm) :	$2.273 \times 10^{12} \text{ cm}^{-3}$
Run 6 (942 ohm-cm) :	$1.475 \times 10^{12} \text{ cm}^{-3}$

It must be mentioned here that the value of electron mobility used in these calculations is the highest reported value. Our layers being not very good, it is expected that mobility may be reduced by as much as two orders of magnitude and hence the actual electron concentration may be higher by the same factor, i.e. of the order of  $10^{14} \text{ cm}^{-3}$ .

## CHAPTER FOUR

SOME STUDIES ON Si-InP HETEROJUNCTIONS4.1 Purpose of This Study

In our experiments, epitaxial layers of InP were grown on Ge and Si substrates, and an attempt was made to study the properties of Si-InP heterojunction diodes, since, to the best of our knowledge, there is no reported work on this topic. Further interest was stimulated by the fact that there is a large lattice mismatch (7.3%) in this pair and a large number of interface states is expected and the effect of these parameters on the properties of heterojunctions could be studied. Also, since the properties of silicon are known in good detail, it was proposed that some idea about the properties of InP could be had through these studies.

Preliminary investigation of the heterojunction behaviour was done on the mechanically polished samples with the help of an IC Wafer Prober (Electroglas Model 131). The copper base-plate and the metal-pin probe served as contacts of the heterojunction. The probe was found to give ohmic contacts, the resistance of which, however, was dependent on the probe pressure. The reproducibility of results was not hampered to a great extent by this mode of making contacts. The I-V characteristics were then displayed on a curve-tracer



(Tektronix Transistor Curve-tracer Type 575). The results are given in Fig. 9(a) - 9(f). It can be seen that with this arrangement the heterojunctions are showing a definite breakdown, although the reverse saturation current is quite high. For further studies the heterojunctions were mounted on transistor headers.

#### 4.2 Fabrication of Heterojunction Diodes

Fabrication of heterojunctions involves making ohmic contacts to the two semiconductors, sawing the chips to proper size, and mounting these chips on headers. Since both Si and InP were n-type, electrodeless Ni-plating solution was used. The ordinary Ni-plating solution, used for elemental semiconductors Si and Ge, does not work effectively on the III-V compounds. Hence, a special plating bath<sup>(22)</sup> was used, which works well on both Si and InP. The solution contained:

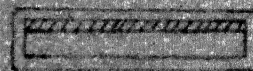
- |  |        |
|--|--------|
| 1. Nickel Chloride ( $\text{NiCl}_2 \cdot 6\text{H}_2\text{O}$ ) | 30 g/l |
| 2. Sodium Hypophosphite  | 20 g/l |
| 3. Ammonium Citrate  | 65 g/l |
| 4. Ammonium Chloride   | 50 g/l |

The colour of this solution is light green and sufficient quantities of  $\text{NH}_4\text{OH}$  have to be added at intervals, to maintain a deep blue colour. This ensures that the pH value of the solution is between 8 and 10. The temperature of the bath has to be controlled at 95-100°C. This was done by putting the

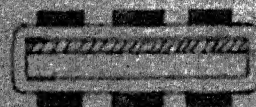
EPITAXIAL LAYER OF INP OVER  
SI SUBSTRATE



NICKEL PLATING



APIEZON WAX DOTS FOR PRESERVING  
SELECTED AREAS OF NI-PLATING



REMOVAL OF EXCESS NICKEL



SAWED CHIP



MOUNTED DIODE  
ON TO-5 HEADER

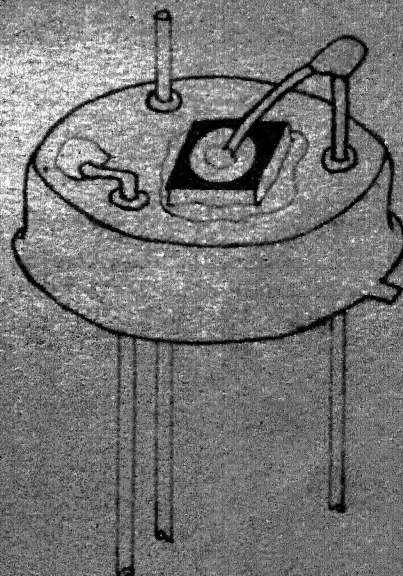


FIG. 8. FABRICATION OF HETEROJUNCTION DIODE

solution in a test-tube which was then submerged in a beaker containing boiling water. Cleaned specimens were then dropped in this test-tube and the plating time needed to give a sufficiently thick Ni layer was about 2-3 minutes. The test-tube was then taken out of the bath and was allowed to cool down to room temperature before the samples were taken out. A shining nickel plating could thus be obtained. To ensure good adhesion of the nickel plating to the semiconductor surfaces, the surfaces were lapped with 5  $\mu$ m alumina lapping powder prior to Ni-plating. Too smooth a surface (e.g., lapped with 1  $\mu$ m powder) gave extremely poor adhesion the plating peeled off very easily.

Suitable areas on the samples were then covered with apiezon wax and the rest of the Ni-plating was dissolved in dilute nitric acid, leaving pairs of spots situated opposite to each other on the two faces of the samples (Fig. 8). The unwanted parts of the samples were then cut-off with a wire saw using a 5mm diameter stainless steel wire and 800 mesh abrasive slurry in glycerine. These chips were cleaned with trichloroethylene to remove all traces of glycerine, and then washed with acetone. Finally the chips were mounted on transistor headers (Type TO-5) by soldering each chip on a separate header. Ordinary soldering wire and a 60 W iron were used.

### 4.3 Measurements

The header was inserted in a test-tube which could be put in different temperature baths. Thus properties of the heterojunction at different temperatures could be studied.

The forward and reverse I-V characteristics were measured at ice point, room temperature, and the temperature of boiling water. For accuracy, a VTVM and a sensitive ammeter were used in conjunction with a stabilised d.c. power supply. The results are given in Fig. 9(g), and are for an n-type Si - n-type InP isotype heterojunction diode.

Figures 9(d) - 9(g) show how the heterojunction characteristics are changing while the sample is going through different stages of processing:

Fig. 9(d) : Before Ni-plating

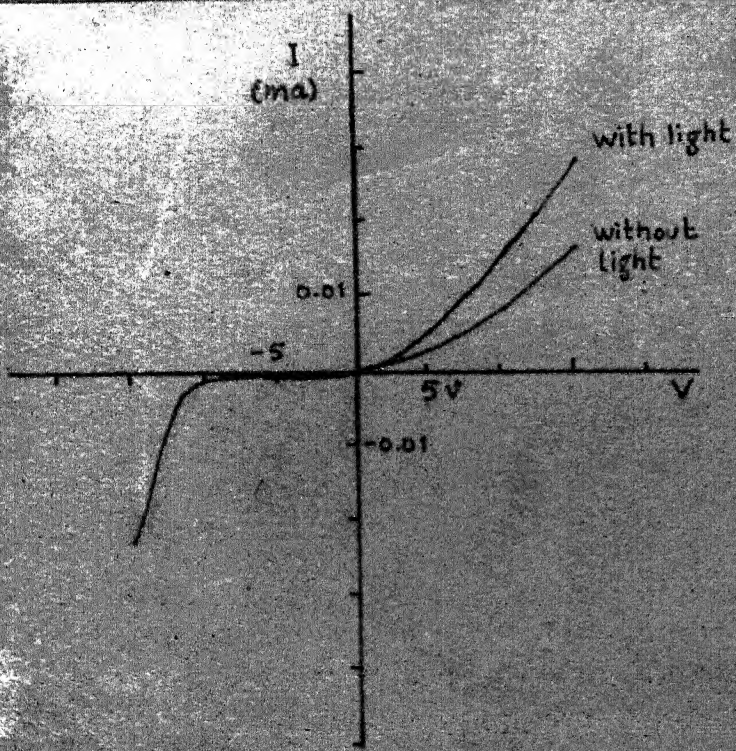
Fig. 9(e) : After Ni-plating and retaining three pairs of  
Ni-dots

Fig. 9(f) : After sawing the sample into three chips

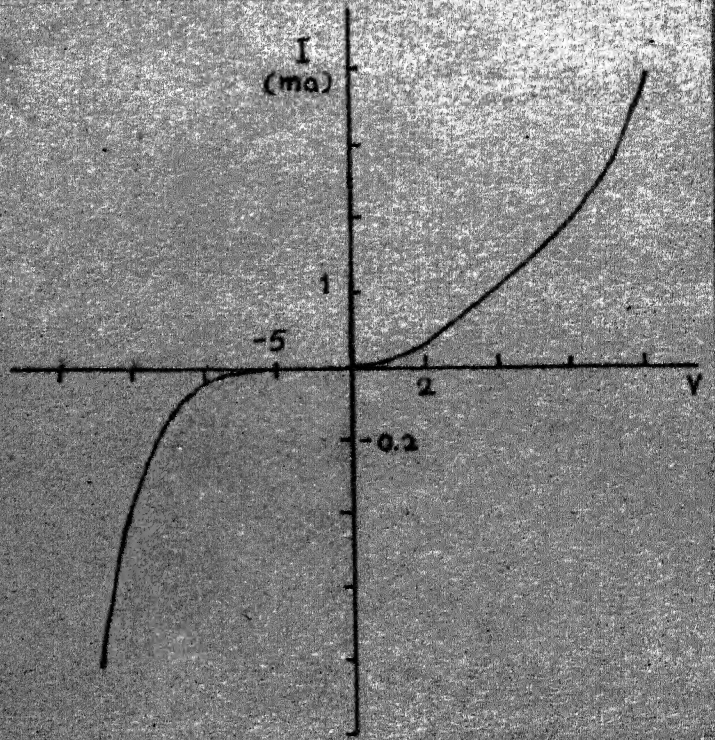
Fig. 9(g) : One of these chips mounted on a header.

The interpretation of the observed I-V characteristics is given in the next chapter.

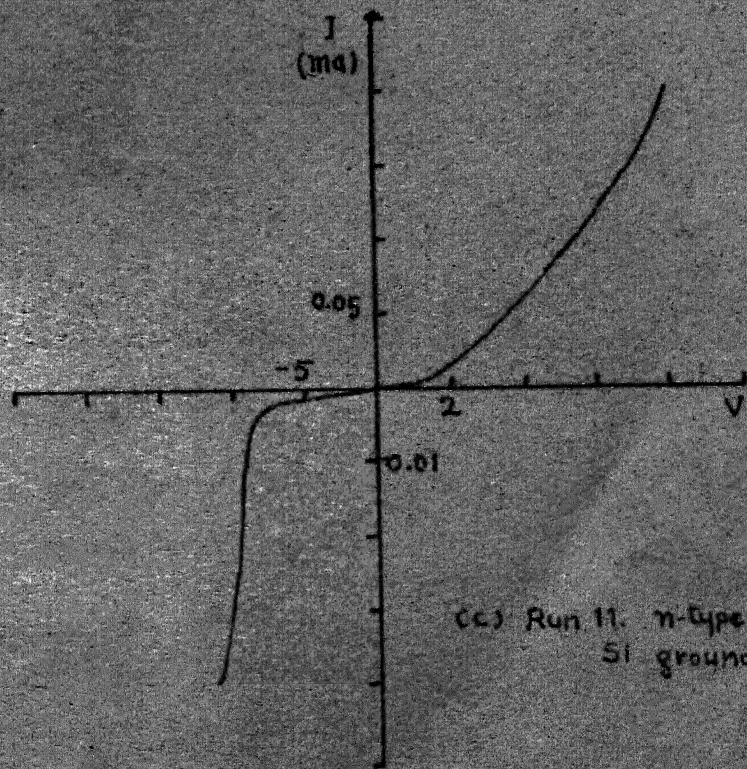




(a) Run 2. p-type Ge-n-type InP.  
InP grounded.



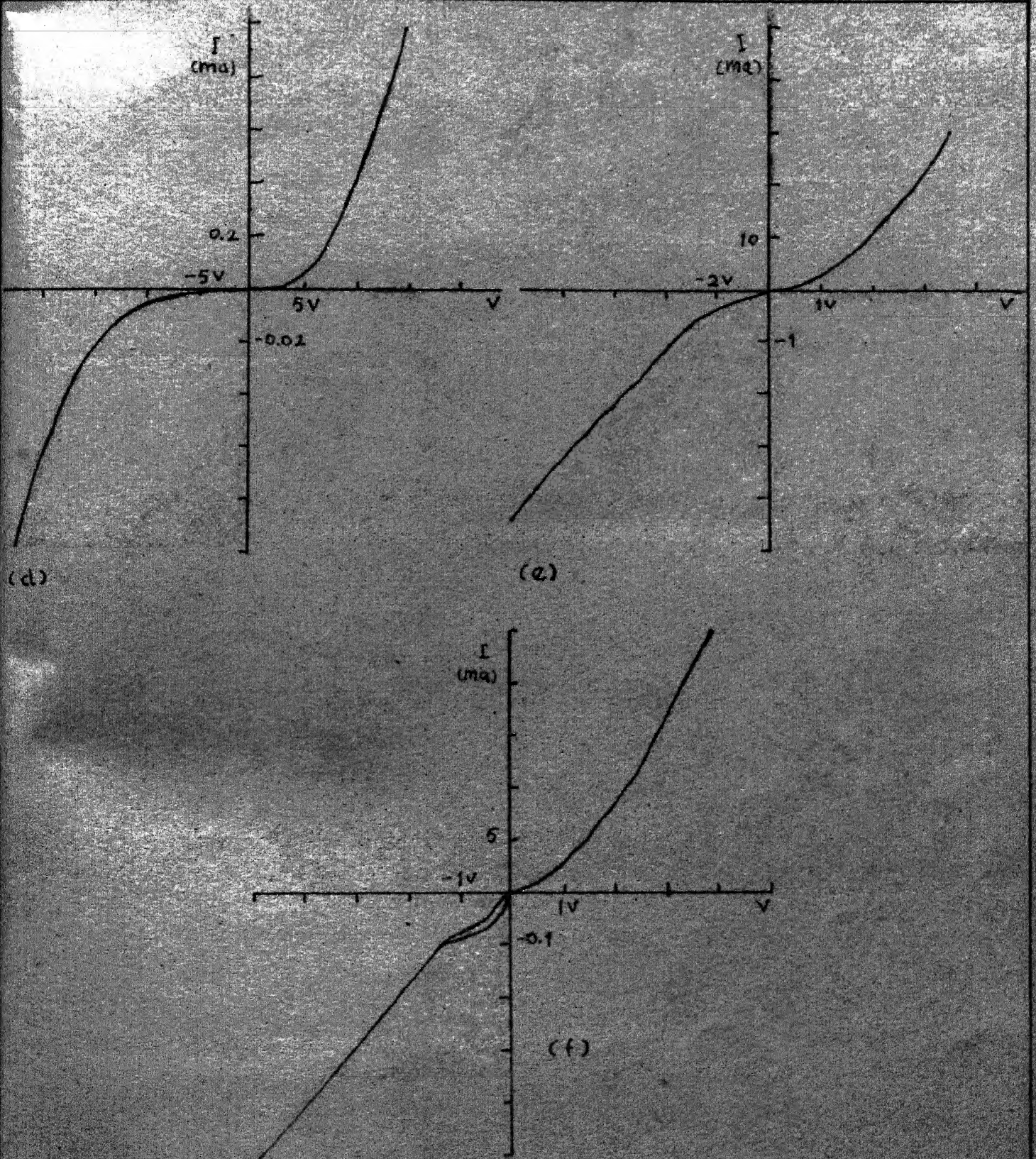
(b) Run 5. n-type Si-n-type InP.  
Si grounded.



(c) Run 11. n-type Si-n-type InP  
Si grounded.

FIG. 9. I-V CHARACTERISTICS OF HETEROJUNCTIONS

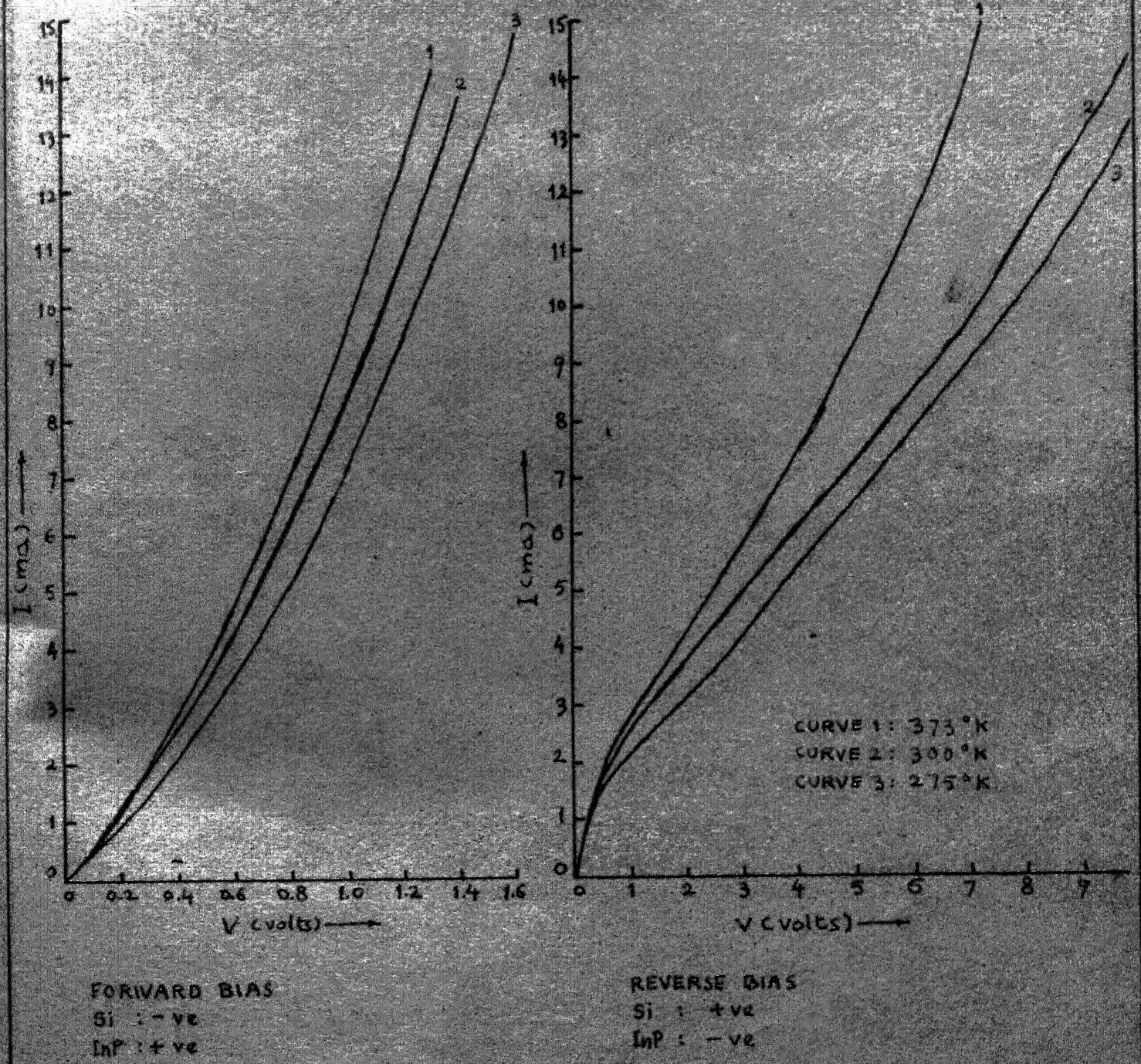




$I$ - $V$  CHARACTERISTICS OF  
n-TYPE SI - n-TYPE INP HETEROJUNCTION (RUN 13)

FIG. 9 (CONTINUED)





(g)

FIG. 9 (CONTINUED) . I-V CHARACTERISTICS OF N-TYPE Si - N-TYPE InP CHIP (RUN 13) MOUNTED ON HEADER: DIODE 12.

## CHAPTER FIVE

## EPILOGUE

5.1 Discussions and Conclusions

The results are presented in Table I.

TABLE I

RUN NO.	SUBSTRATES	EPITAXIAL LAYERS
2	<p>(i) <u>Silicon</u>  n-type,  Orientation: (1 1 1)  Thickness: 10 mil  Dislocation  Density: <math>5 \times 10^5 \text{ cm}^{-2}</math>  Temperature: 650°C</p> <p>(ii) <u>Germanium</u>  p-type  Orientation: (1 1 0)  Thickness: 10 mil</p> <p>(iii) <u>Quartz</u>  Thickness: 10 mil  Temperature: 630°C</p>	<p>Colour: Dark gray with tary lusture  Thickness on Ge: 16 <math>\mu\text{m}</math>  Surface texture: non-uniform layers with whisker like growth  Conductivity type: n  Resistivity: 610 ohm-cm  p-type Ge - n-type InP aniso-type heterojunction  Behaviour: Fig. 9(a)  Adhesion: moderate</p>
5	<p>(i) <u>Quartz</u>  10 mil  675°C</p> <p>(ii) <u>Silicon</u>  n-type, 1 ohm-cm  (1 1 1)  8 mil  <math>2 \times 10^6 \text{ cm}^{-2}</math>  660°C</p>	<p>Adhesion: poor  Thickness on quartz: 13 <math>\mu\text{m}</math>  Thickness on Si : 15 <math>\mu\text{m}</math>  Whisker like growth.  n-type Si-n-type InP hetero-junction behaviour: Fig. 9(b).</p>

RUN NO.	SUBSTRATES	EPITAXIAL LAYERS
6	<p>(i) <u>Quartz</u> 10 mils 660°C</p> <p>(ii) <u>Silicon</u> p-type, 1 ohm-cm (1 1 1) 10 mil <math>8 \times 10^4 \text{ cm}^{-2}</math> 640°C</p> <p>(iii) <u>Germanium</u> p-type, 1 ohm-cm (1 0 0) 15 mil 610°C</p>	<p>Substrates kept parallel to the gas stream</p> <p>Uniform layers</p> <p>Good adhesion</p> <p>Some indium inclusions on the surface</p> <p>Thickness on Si: 23 <math>\mu\text{m}</math></p> <p>Resistivity: <del>1.32</del> 1.32 ohm-cm</p> <p>Infra-red absorption: Fig. 7(a)</p> <p>Lattice parameter: 5.8344 Å</p>
7	<p>(i) <u>Sapphire</u> 81.5 mil (0 0 0 1) basal plane 660°C</p> <p>(ii) <u>Silicon</u> n-type, 1 ohm-cm (1 1 1) 10 mil <math>4 \times 10^6 \text{ cm}^{-2}</math> 660°C</p>	<p>Uniform layers with moderate adhesion and some indium inclusions.</p> <p>Thickness on Si: 12.5 <math>\mu\text{m}</math></p> <p>Dislocation density on Si: <math>5 \times 10^6 \text{ cm}^{-2}</math></p>
8	<p>(i) <u>Quartz</u> 10 mil 630°C</p> <p>(ii) <u>Germanium</u> p-type, 1 ohm-cm (1 0 0) 20 mil 660°C</p>	<p>Layers: uniform on quartz but not on Ge.</p> <p>Adhesion: moderate</p> <p>Inclusions: no phosphorous but some indium inclusions.</p> <p>Thickness on Ge: 20 <math>\mu\text{m}</math></p>

RUN NO.	SUBSTRATES	EPITAXIAL LAYERS
11	(i) <u>Sapphire</u> 81.5 mil (0 0 0 1) 630°C (ii) <u>Quartz</u> 8 mil 630°C (iii) <u>Silicon</u> n-type, 1 ohm-cm (1 1 1) 8 mil 615°C 4 x 10 <sup>6</sup> cm <sup>-2</sup>	Uniform layers with moderate adhesion Thickness on Si: 17 μm Dislocation Density on Si: 8 x 10 <sup>7</sup> cm <sup>-2</sup> Infra-red absorption: Fig. 7(b), (c) Lattice parameter: 5.876 Å n-type Si - n-type InP heterojunction behaviour: Fig. 9(c)
12	<u>Silicon</u> n-type, 1 ohm-cm (1 1 1) 10 mil Three wafers at 615, 625 and 635°C respectively	Uniform layers Adhesion: poor in some areas but moderate otherwise Thickness on Si substrate kept at 615°C: 16 μm Resistivity of substrate kept at 625°C: 140 ohm-cm
13.	(i) <u>Silicon</u> n-type, 1 ohm-cm (1 1 1) 10 mil (ii) <u>Silicon</u> p-type, 1 ohm-cm 10 mil	Nonuniform layers with moderate adhesion Thickness: 40 μm Resistivity: 140 ohm-cm n-type Si - n-type InP hetero- junction behaviour: Fig. 9(d)- (g)



- (1) From the infra-red measurements shown in Fig. 7(a), we see that the material deposited on the sapphire substrate (from run no. 6) is a semiconductor with a band-gap energy being somewhere in the range 1.24 to 1.4 eV. The reported value of  $E_g$  for InP is 1.33 eV.
- (2) The measured values of lattice parameter of this material, as given in table II, show fair agreement with the reported value for InP.
- (3) From these facts it can be concluded that these epitaxial layers are really of indium phosphide.

But at the same time it is also seen that these layers are of extremely poor quality. This is illustrated by:

- a. Peeling off of epitaxial layers.
- b. The infra-red spectrum in Fig. 7(c) indicates that there is a metal (most probably indium) layer on the substrate. It may be said here that although in run no. 14, only scarce and highly non-uniform indium deposits were found, not much can be concluded from this run alone. There is no guarantee that in other runs (e.g., in run no. 11 which gives the infra-red spectrum shown in Fig. 7(c).) the surface density of In deposits is not high, i.e., there might have been a uniform layer of In on this particular substrate. But on the other hand, it can not also be concluded that a metal layer is present in all other samples.

c. Although no intentional doping was done, still all the epitaxial layers were n-type. Fig. 7(b) indicates that the donor level is approximately 0.1 eV below the conduction band edge. This n-type doping might have been caused by the remaining oxygen impurities in the gas stream. The possibility of doping by other impurities can not also be ruled out. These impurities may come from<sup>(21)</sup> the hydrogen stream itself, or from  $\text{PCl}_3$ , which is impure by semiconductor standards, or from the reaction tube, indium boat, and the quartz substrate holders. There is also a possibility of contamination from the PVC tubing, copper bed,  $\text{CaCl}_2$  and  $\text{P}_2\text{O}_5$  columns, and glass-wood.

(4) The back reflection Laue photograph indicates that the epitaxial layer, at least at the spot where the X-ray beam was falling, is single crystalline. This may be true for other parts and other samples also, since the growth rate was kept very low to promote single crystal growth.

(5) Figures 9(d) - 9(g) show that the heterojunction characteristics are changing with processing. It can be noted that the probe gives a high resistance contact and also changes the nature of the characteristics. Curves in Fig. 9(d) were obtained directly on the polished epitaxial layer, before Ni-plating. With Ni-plating, Fig. 9(e), the contact resistance has abruptly decreased, which is expected. When this chip is soldered on a header, the contact resistance is further reduced. Here, the



change in the reverse characteristics is more than the change in the forward one. It is also seen that there is a vast difference in the curves given in Fig. 9(d) and in fig. 9(g). The reverse characteristics in Fig. 9(d) bears the semblance of a soft breakdown, which is totally absent in Fig. 9(g); in the forward characteristic of the sample the current starts-off after about 2.5 volts, but for the mounted diode this forward current is monotonously increasing with voltage right from the origin.

It may possibly be concluded from the foregoing discussion that the soft-breakdown observed with the probe contact may be a result of surface impurities or a bad contact.

## 5.2 Suggestions

This work was rather exploratory and was carried out to find out whether epitaxial growth is at all possible with the existing set-up, and what are all the difficulties. As could be anticipated, existing literature was of almost no help. It all turned out to be more of an art than science. This study is thus highly empirical in nature. On the basis of our experience gained during this work, we make the following suggestions:

1. More detailed study of growth parameters is necessary in order to:
  - (a) discourage In layer growth,

- (b) give good adhesion, and
  - (c) give uniform epitaxial layers.
2. Deposition of InP on semi-insulating InP substrates is recommended.
  3. An entirely new system should be built which features a two-zone furnace, palladium diffuser, high-purity starting materials, and has provisions for later additions which may include an  $\text{AsCl}_3$  bubbler. This can render the system versatile enough to study the ternary systems like  $\text{In}(\text{As}, \text{P})$ ,  $(\text{In}, \text{Ga})\text{P}$  or in general  $(\text{In}, \text{Ga})(\text{As}, \text{P})$ .
  4. Effect of intentional n-type doping should be studied. This would be necessary for further device work.
  5. P-N junctions can be fabricated at a later stage when a fairly good control over n-type doping has been achieved. This would open up vast prospects for work in the area of Light Emitting Diodes etc.

TABLE II  
X-RAY ANALYSIS BY DEBYE-SCHERRER TECHNIQUE

MATERIAL: Wall deposit from runs 11, 12 and 13. Camera Dia: 114.6 mm Radiation: CuK (1.5418 Å) Exposure time: 5 hours KV : 30, mA : 26					MATERIAL: Scratchings from substrate holder in run 6. Camera Dia: 57.3 mm Radiation: CuK Exposure time: 4 hours KV : 30, mA : 26			
No.	$\theta$ , in degrees	d, in Å	plane (hkl)	Lattice parameter Å	$\theta$ , in degrees	d, in Å	plane (hkl)	Lattice parameter Å
1	26.3	1.7384	311	5.764	22.05	2.0526	220	5.80396
2	30.625	1.5120	-	-	26.55	1.7232	222	5.959
3	39.35	1.2148	422	5.9356	30.7	1.5089	-	-
4	43.775	1.1134	511	5.764	36.4	1.2980	-	-
5	46.575	1.06055	440	5.9963	39.74	1.2048	422	5.81385
6	51.800	0.98014	600	5.8813	44.2	1.1048	511	5.7394
7	54.30	0.94849	620	5.997	46.8	1.0566	440	5.9598
8	63.575	0.8601	444	5.9581	51.95	0.97815	531	5.786
9	69.50	0.82232	711	5.8703	60.7	0.88324	533	5.79
10					70.2	0.81864	711	5.8455
11					80.75	0.78039	-	

Average lattice parameter:

5.876 Å

Average lattice parameter:

5.8344 Å

Standard value of lattice parameter of InP: 5.86875 Å

% error: 0.123

% error: 0.58

## REFERENCES

1. Gunn, J.B.: IBM J. Res. Dev., 8, 141-59 (1963).
2. Neuberger, M.: Handbook of Electronic Materials, Vol. 2, III-V Semiconducting Compounds, IFI/Plenum (1971).
3. Hilsum, C. and Rees, H.D.: Electron. Lett., 6, 277-8 (1970).
4. "Semiconducting Compounds", J. Applied Physics, June 1961.
5. Dean, P.J.: Trans. Met. Soc. AIME, 242, 384-4000 (1968).
6. Wieder, H.H.: J. Vac. Sci. Technol., 8, 210-223 (1971).
7. Kramer, B., Maschke, K. and Thomas, K.: Phys. Status Solidi B, 48, 635-42 (1971).
8. Hilsum, C. and Rose-Innes, A.C.: Semiconducting III-V Compounds, Pergamon Press, London (1961).
9. Willardson, R.K. and Goering, H.L.: Compound Semiconductors, Vol. 1: III-V Compound semiconductors Reinhold (1961).
10. Madelung, O.: Physics of III-V Compounds, Wiley, New York, (1964).
11. Willardson, R.K. and Beer, A.C., Eds.: Semiconductors and Semimetals, Vol. 1 to 4, Academic Press (1964-1968).
12. Wieder, H.H.: Intermetallic Semiconducting Films, Pergamon Press (1970).
13. Ehrenrich, H.: Phys. Rev., 120, 1951-3 (1960).
14. James, L.W. et al., Phys. Rev. B, 1, 3998-4004 (1970).
15. Colliver, D. and Prew, B.: Electronics, 45, 110-3 (1972).

16. Clarke, R.C., Joyce, B.D. and Wilgoss, W.H.E.: Solid State Commun., 8, 1125-8 (1970).
17. Hamiuddin, M.: M.Tech. Thesis, Interdepartmental Programme in Materials Science, I.I.T., Kanpur, July 1973.
18. Willardson and Goering, Ref. 9, Page 448.
19. Gatos, H.C. and Lavine, M.C.: J. Electrochem. Soc., 107, 427 (1960).
20. Kane, P.L. and Larrabee: Characterization of Semiconductor Materials, McGraw Hill, New York (1970).
21. Eaves, L. et al.: J. Phys. C, 4, 42-7 (1971).
22. Daw and Mitra: Solid State Electron., 8, 697-8 (1965).
23. Hope, D.A.: Environmental Engng., 35, 9-12 (1968).